7A.4

Observations of K_{dp} in the ice region of precipitating clouds at X-band and C-band radar frequencies

R. Bechini[1,3]*, L. Baldini[2], V. Chandrasekar[3], R.Cremonini[1], E. Gorgucci[2]

[1]Arpa Piemonte, Torino, Italy
[2]Institute of Atmospheric Sciences and Climate - CNR, Roma, Italy
[3]Colorado State University, Fort Collins CO 80523

1. INTRODUCTION

Specific differential phase (K_{dp}) signatures in the ice region of convective storms have traditionally been attributed to the effects of ice particle electrification (Caylor and Chandrasekar, 1996). More recently, positive values of specific differential phase shift (K_{dp}) in the ice region of precipitating clouds have been shown to be linked to increased surface precipitation rates at S-band (Kennedy and Rutledge, 2011). The regions of enhanced K_{dp} are observed near the -15℃ isotherm and are likely related to the growth of plate-like crystals. The observed values of specific differential phase shift are only few tenths of deg/km at S-band, but due to the K_{dp} scaling with frequency, are expected to be higher and more easily detectable at higher frequencies.

High resolution RHI scans collected by the X-band dual polarization transportable system of ARPA Piemonte (ARX) during stratiform precipitation, for example, revealed extended regions with K_{dp} values above 1.5 deg/km in the mid-tropospheric layer at 5-7 km height, corresponding to temperatures in the range –9C to –20C as measured by nearby radio sounding (Fig. 1).

This study aims at characterizing the phenomenological behavior of K_{dp} in the ice region of mesoscale precipitation systems simultaneously observed at C-band and X-band radar frequencies (5.640 and 9.375 GHz respectively). For this study the C-band measurements were collected by the operational C-band dual polarization of ARPA Piemonte located in Bric della Croce, close to Turin, and by the ARX, located in Carmagnola at 16-km distance from the C-band radar (fig. 2). The C-band radar is on the top of a hill at 740m MSL, while the X-band is over the plains at 235 m MSL.

The operational polarimetric C-band radar allowed an extensive analysis of K_{dp} vertical profiles in the North-West Italy subalpine region.

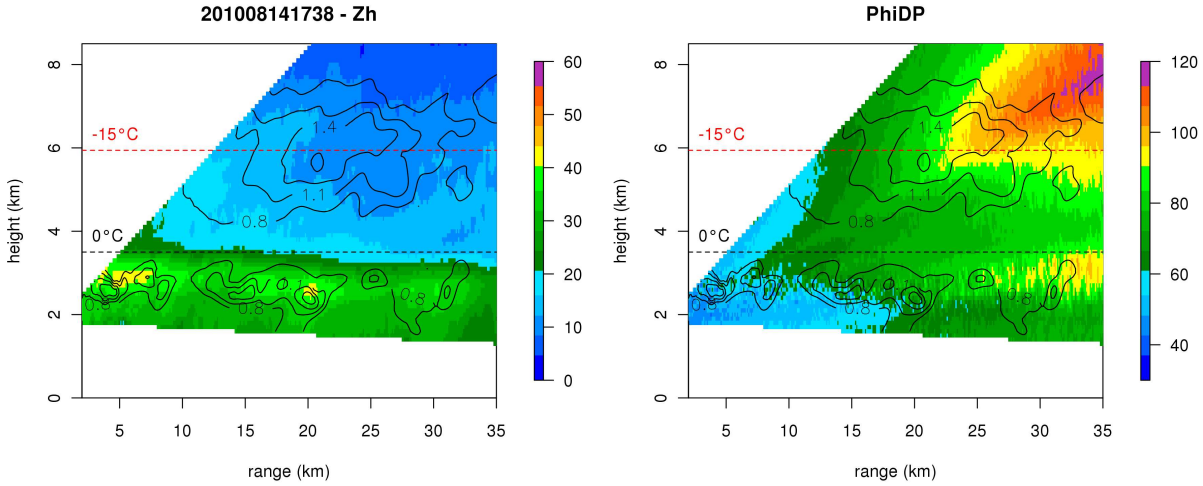

Figure 1. X-band RHI during the 2010 Summer campaign on the mountains in South-Western Piemonte (2010-08-14, 17:38UTC, radar at 1835 m MSL, Colle di Tenda). Left: reflectivity corrected for attenuation in rain. Right: Φ_{DP}. The K_{dp} contour lines (0.8 to 1.7 deg/km) are overplotted on both panels.

* Corresponding author address: Renzo Bechini, Arpa Piemonte, Via Pio VII, 9, 10135 Torino, Italy; e-mail: r.bechini@arpa.piemonte.it

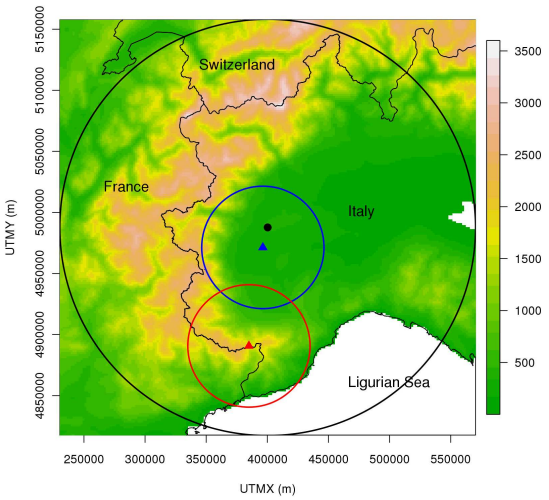

Figure 2. North-western Italy topography with location and range of the radars: Bric della Croce (C-band, filled black circle), ARX at Colle di Tenda (red triangle, RHI in fig. 1), ARX at Carmagnola (blue triangle, see section 4).

2. VERTICAL PROFILES STATISTICS FROM C-BAND RADAR OBSERVATIONS

More than one year of data routinely collected between 2009 and 2011 by the operational C-band radar have been analyzed, leading to a selection of 64 significant rain events (>5 mm daily cumulated precipitation in at least one rain-gauge in the area of interest). Only events in which the freezing level was above 2 km MSL were considered, in order to allow a meaningful comparison with the lowest level reflectivity. The events are classified as stratiform or convective based on the daily vertical profile of reflectivity (VPR).

Figure 3 shows a typical daily vertical profiles of reflectivity and its vertical derivative (left panel, black and blue lines, respectively) and of K_{dp} (right panel), the latter estimated using the adaptive technique of Wang and Chandrasekar (2010), for a stratiform event.

The vertical profiles are calculated considering, for all the radar volumes of the event, collected with a 10-minute frequency, sweeps at elevation angles below 15 degrees and range bins within 50 km from the radar to avoid excessively sparse vertical sampling. The data are then binned in 0.2 km depth height levels. A marked K_{dp} peak, centered around the -15℃ level, can be seen . The K_{dp} peak appears just below a local maximum in the height derivative of the reflectivity. According to Lo and Passarelli (1982), the increased height derivative of reflectivity may be interpreted as an indication of the transition from vapor deposition to aggregation processes. Although aggregation normally occurs above -5℃, a secondary maximum between -10 and -16℃ may exist when the arms of the dendritic crystals become entangled (Houze, 1993). The high values of K_{dp} were explained by Kennedy and Rutledge (2011) in terms of the dominance of plate-like crystals grown by vapor deposition.

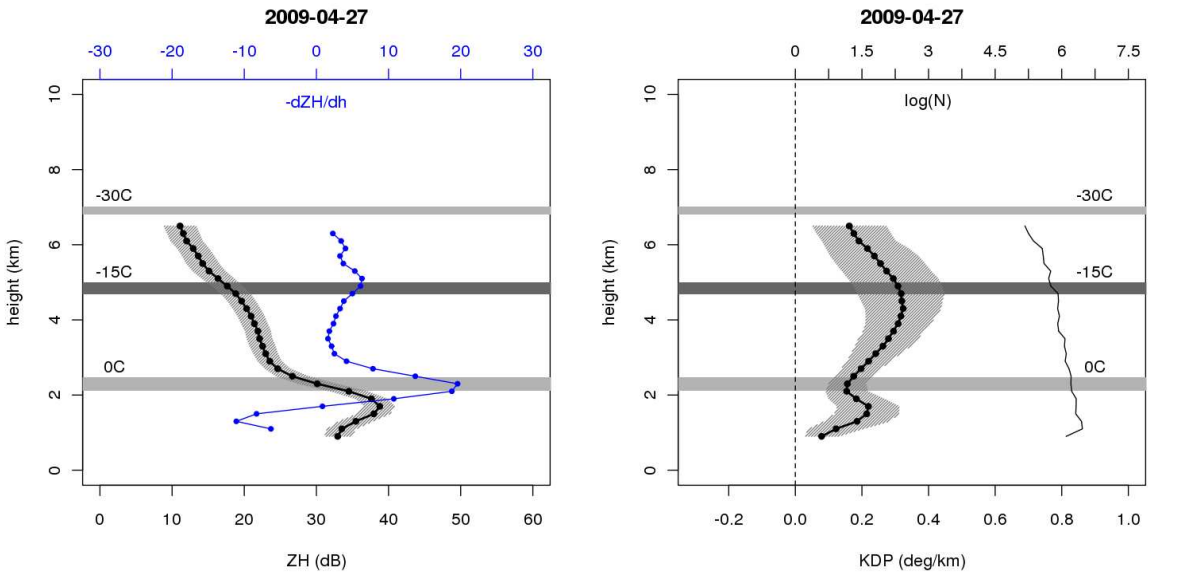

Figure 3. Examples of daily average vertical profiles of reflectivity (left; the blue line is the height derivative of reflectivity) and K_{dp} (right) for a stratiform precipitation case (27 April 2009). The gray area represents one standard deviation. The horizontal gray stripes represent the daily min/max height of the corresponding temperature value from the Italian limited area model model LAMI (www.cosmo-model.org). The solid line without symbols in the right panel shows the number of data averaged in the profiles (log scale on the top axis).

3. ELECTROMAGNETIC SCATTERING SIMULATIONS

T-matrix simulation of scattering have been performed to interpret radar measurements at the -15℃ isotherm level. Simulations follow the approach adopted by Kennedy and Rutledge (2010), modelling particle population at that level as mix of plate-like crystals for diameter smaller than 3 mm and aggregates for larger diameters and deriving S-, C- and X-band radar parameters for different exponential particle size distributions (PSD). Both components are modelled as mixture of ice and air (the Bruggeman's effective medium approximation is used), but differ both in aspect ratio and in density.

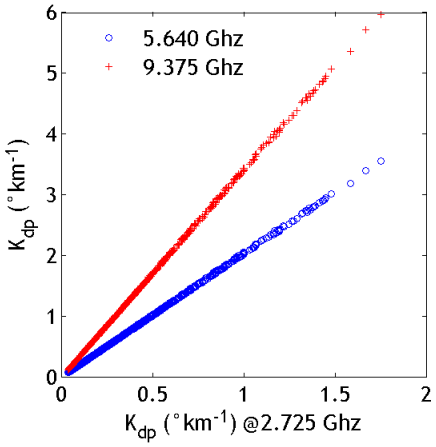

Figure 4. Electromagnetic scattering simulations of K_{dp} for aggregates/plates mixture at -15℃

Plate-like ice-particle are modelled as oblate spheroid (aspect ratio varying between 0.05 and 0.15) with high density (as a function of diameter according to Heymsfield 1972). Conversely, aggregates were modelled as amost sperical ellipsoid (aspect ratio of .85) and low density (~0.15 g cm^{-3}). It is easy to verfy that both K_{dp} and IWC are almost entirely determined by the characteristics of plate-like particles. Fig. 4 reports simulations obtained at -15℃ temperature, at the frequenceies of 2.725 Ghz (S-band), 5.64 Ghz (Bric della Corce, C-band), 9.375 (X-band, ARX). The PSD is assumed to follow an exponential distribution whose parameters N_0, Λ vary in a wide range, namely, with $\log_{10}(N_0)$ uniformly distributed between $\log_{10}(5x10^3$ mm^{-1} m^{-3}) and $\log_{10}(40$ x10^3 mm^{-1} m^{-3}), while $1/\Lambda$ varies between 1/2.5 and 1/4.5 cm.

Simulations show that Z_h and Z_{dr} values are not influenced by the frequency, whereas K_{dp} can be scaled according to the ratio of wavelengths. As stated before, most of the IWC is provided by the high density plates of the PSD. Simulations indicates that IWC is fairly linerly related to K_{dp}, whereas a power law can be established between Z_h (mm^6 m^{-3}) and IWC (g cm^{-3}). Fig. 5 illustrates the correspoding scatterplots at C-band. It should be noticed that the linear algorithm based on K_{dp} has a normalized standard error lower than 10%.

4. CROSS-VALIDATION WITH COINCIDENT C- AND X-BAND RADAR OBSERVATIONS

The above scattering simulations results are validated with radar observations of K_{dp} at C- and X-band collected by the Bric della Croce and ARX radar at Carmagnola, for an intense widespread rainy event occurred on 27 April 2009. Southerly moist flow caused continuous rain for most of the day with 24 hours average accumulation of 76 mm over the plains, with peak values up to 140 mm.

The X-band radar performed a strategy that included a 90-deg elevation PPI within each 5-min volume scan. An analysis of the Doppler velocity vertical looking observations allows to infer that riming was likely not relevant for this event, at least in the vicinity of the radar. The dominant Doppler velocity can be taken as representative of the particle fall speed, since vertical motions typically of the order of few tenths m/s should average to near 0 m/s over the day. The lack of a significant number of particles with fall speed in excess of 1.5 m/s is here taken as a proof of the insignificance of riming accretion processes (Zawadski et al. 2001).

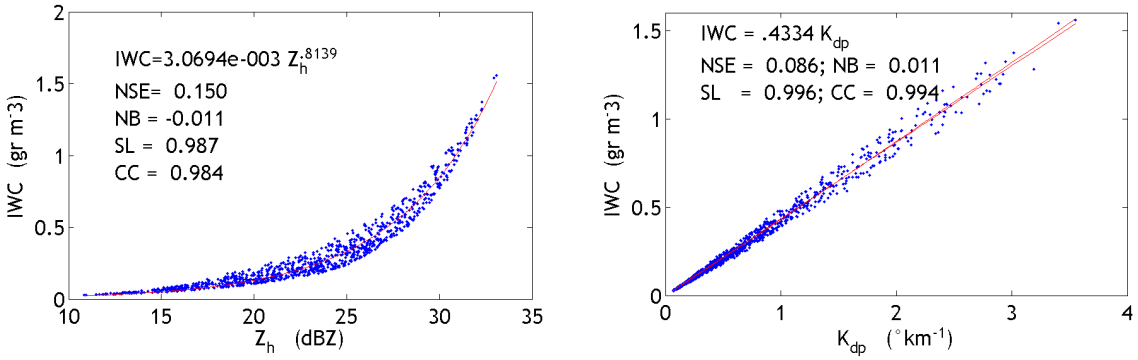

Figure 5. IWC as a function of Z_h (left) and K_{dp}(right). Results are obtained using the same simulation used for the scatterplot in Fig. 4 at C band. Shown are algorithms for IWC at C-band with the corresponding merit figures.

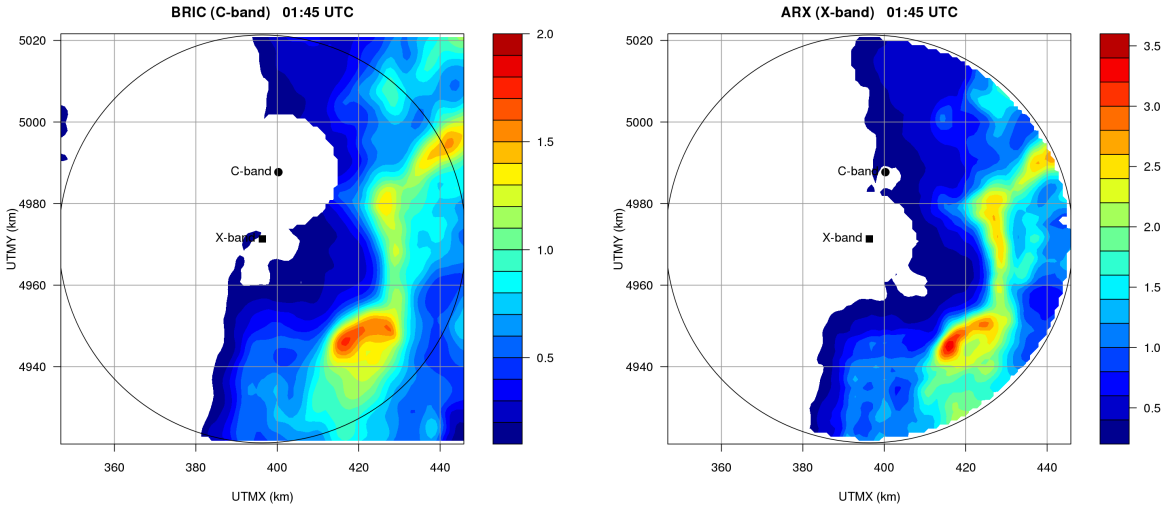

Figure 6. Average K_{dp} in the layer 4200-5500 m MSL (around -15C), at minute 495, 01:45 UTC. Left: C-band radar. Right: X-band. The circle in both panels represents the 50 km domain of the X-band radar.

The radar observations are therefore considered suitable for comparison with the scattering simulations of ice particle distributions resulting from vapor deposition and aggregation processes only.

Fig. 6 shows an example of the average K_{dp} field in the layer 4200-5500 m MSL (centered around -15℃) f or C- band (left) and X-band radar (right). The agreement between the two radar estimates is remarkable, thanks also to the proximity of the two systems (16 km). The X-band K_{dp} estimates show some more detail due to the higher range resolution (125 m) compared to the C-band (340 m).

In general K_{dp} at X-band is observed to be about 1.7 times higher than K_{dp} at C-band, in good agreement with the ratio of the operating frequencies of the two radars. Peak values of observed K_{dp} during the event are 1.7 deg/km at C-band and 3.4 deg/km at X-band. Such values are explainable by the scatterplot of Fig. 4.

When K_{dp} values are well above noise (i.e. K_{dp} > 0.2 deg/km at C-band), K_{dp} fields at C- and X-band are highly correlated (r>0.9), indicating the robustness of the K_{dp} estimates in the ice region. Reflectivity instead show poorer correlation (0.7<r<0.9) likely due to PSD variability and to path attenuation uncertainties (in rain and melting layer), or attenuation induced by radome wetting (Bechini et al., 2010), while non-Rayleigh scattering influence is excluded based on T-matrix simulations.

5. CONCLUSIONS

The behavior of high K_{dp} in the ice region dominated by vapor deposition growth is examined. The high K_{dp} values near the -15℃ level previously examined by Kennedy and Rutledge (2010) for snowfall events are here shown to be a rather common attribute of stratiform precipitation, independently of the freezing level height. This is confirmed experimentally by comparison of coincident C-band and X-band radar measurements in Italy. In fact, electromagnetic scattering simulations show that K_{dp} scales with radar operating frequency

Further investigation will aim at a better representation of the ice microphysics of stratiform precipitation, also through the use of differential reflecivity measurements, that were not considered in this study. In addition, possible adaptation of the K_{dp} estimation algorithm may be seeked in order to improve the performance at the low intensities typical of widespread precipitation systems.

Acknowledgements

Participation of V. Chandrasekar is supported by the NSF ERC program.

6. REFERENCES

Bechini, R., V.Chandrasekar, R. Cremonini, S. Lim, 2010: Radome attenuation at X-band radar operations. Proc of the European Conference on radar Meterol and Hydrol ERAD 2010 [on line: http://www.erad2010.org/pdf/POSTER/Thursday/02_Xband/01_ERAD2010_0346_extended.pdf]

Caylor, I.J., and V. Chandrasekar, 1996: Time-varying ice crystal orientation in thunderstorms observed with multiparameter radar. IEEE Trans. Geosci. Remote Sensing, 34, 847-858.

Heymsfield, A., 1972: Ice crystal terminal velocities. J. Atmos. Sci., 29, 1348–1357.

Houze, R. A., Jr., 1993: Cloud Dynamics. Academic Press, 573 pp.

Kennedy, P. C., S. A. Rutledge, 2011: S-band dual-polarization radar observations of winter storms. J. Appl. Meteor. Climatol., 50, 844–858.

Lo, K. H., and R. E. Passarelli Jr., 1982: The growth of snow in winter storms: An airborne observational study. J. Atmos. Sci., 39, 697–706.

Wang, Y., and V. Chandrasekar, 2009: Algorithm for the estimation of specific differential phase. J. Atmos. Oceanic Technol., 26, 61–78.

Zawadzki, I., Fabry, F., and Szyrmer, W. 2001. Observations of supercooled water and of secondary ice generation by a vertically pointing X-band Doppler radar. Atmospheric Research 59-60, 343-359.